Electromagnetic Cylindrical Transparent Devices with Irregular Cross Section

Cheng-fu YANG[1, 2], Jing-jing YANG [1, 2], Ming HUANG[1], Ji-hong SHI[1], Jin-hui PENG[2]

[1]School of Information Science and Engineering, Yunnan University, Kunming 650091, PR China
[2]Faculty of Metallurgical and Energy Engg., Kunming Univ. of Science and Technology, Kunming 650093, PR China

huangming@ynu.edu.cn

Abstract. *Electromagnetic transparent device is very important for antenna protection. In this paper, the material parameters for the cylindrical transparent devices with arbitrary cross section are developed based on the coordinate transformation. The equivalent two-dimensional (2D) transparent devices under TE plane and cylindrical wave irradiation is designed and studied by full-wave simulation, respectively. It shows that although the incident waves are distorted in the transformation region apparently, they return to the original wavefronts when passing through the device. All theoretical and numerical results validate the material parameters for the cylindrical transparent devices with arbitrary cross section we developed.*

Keywords

Transparent device, transformation optics, metamaterials, finite element method.

1. Introduction

Control of electromagnetic wave with metamaterials is of great topical interest, and is fuelled by rapid progress in electromagnetic cloaks [1-6]. Cloaking techniques rely on the transformation of coordinates, e.g., a point in the electromagnetic space is transformed into a special volume in the physical space, thus leading to the creation of the volume where electromagnetic fields do not exist, but are instead guided around this volume [7]. Based on the coordinate transformation idea, some interesting optical and microwave applications, such as invisibility cloaks [8-10], illusion device [11], concentrators [12, 13], rotation cloaks [14], electromagnetic wormholes [15], impedance matched hyperlenses [16], field shifters [17], anti-cloaks [18], super-scatterers [19], superabsorbers[20], remote cloaks [21], cloaking sensor [22], transparent device [23], have been proposed. Among various novel applications, transparent device is an important device for antenna protection. Recently, Yu et al. [23] proposed a kind of transformation method of compress or stretching, and designed the circular and elliptical transparent devices with relatively high symmetry. However, to best of our knowledge, there is no report about the cylindrical transparent devices with irregular cross section.

Inspired by the work of Li et al. [8], we propose and design the 2D transparent devices with non-conformal inner and outer boundaries. Based on coordinate transformation method, the general material parameter tensors for the 2D transparent devices are developed, and validated by numerical simulation. Results show that the performance of the 2D transparent device is independent on the orientation of the incident electromagnetic wave; deviation of material parameters from perfect 2D transparent device results in a mismatching of impedance and gives rise to a distortion of the electrical field in the forward-scattering region. The material parameters developed in this paper can be also specialized to the 2D transparent devices with conformal inner and outer boundaries or regular shapes, such as circular, elliptical and square, which represents an important progress towards the realization of arbitrary shaped 2D transparent devices.

2. Theoretical Model

According to the coordinate transformation method, the permittivity $\varepsilon^{i'j'}$ and permeability $\mu^{i'j'}$ tensors of the transformation media can be written as [24]

$$\begin{cases} \varepsilon^{i'j'} = \Lambda_i^{i'} \Lambda_j^{j'} \left|\det(\Lambda_i^{i'})\right|^{-1} \varepsilon^{ij} \\ \mu^{i'j'} = \Lambda_i^{i'} \Lambda_j^{j'} \left|\det(\Lambda_i^{i'})\right|^{-1} \mu^{ij} \end{cases} \tag{1}$$

where $\Lambda_i^{i'}$ is the Jacobian transformation matrix, $\left|\det(\Lambda_i^{i'})\right|$ is the determinant of the matrix, ε^{ij} and μ^{ij} are the permittivity and permeability of the original space, respectively. The transformation is identified along the z axis, and the coordinate transformations for the 2D transparent device with arbitrary geometry are in the *xoy* plane. The transformed coordinate schematic diagram is shown in Fig. 1, where four cylinders with arbitrary cross section enclosed by contours $R_1(\varphi)$, $R_2(\varphi)$, $R_3(\varphi)$, and $R_4(\varphi)$, divide the space into four regions S_1, S_2, S_3 and S_4. $R_n(\varphi)$, can be chosen as arbitrary continuous functions with period 2π, and it can be expressed by a Fourier series as [8]

$$R_n(\varphi) = \sum_{m=0}^{\infty} A_m \cos(m\varphi) + \sum_{m=1}^{\infty} B_m \sin(m\varphi) \cdot \quad (2)$$

The coordination transformation for the transparent devices with arbitrary geometries includes two steps [23]. Firstly, we keep the regions S_1 and S_4 invariant; secondly, we compress the region S_3 and S_4 into region S_4, and stretch the region S_2 to the region S_2 and S_3. The corresponding mapping is,

$$r' = k_1 r + k_2 , \quad (3)$$

$$\varphi' = \varphi , \quad (4)$$

$$z' = z \quad (5)$$

where

$$k_1 = (\tau - R_3(\varphi))/(\tau - R_2(\varphi)) ,$$

$$k_2 = \tau(1-k_1) = \tau[R_3(\varphi) - R_2(\varphi)]/[\tau - R_2(\varphi)] \cdot$$

If $R_3(\varphi) < r < R_4(\varphi)$, $\tau = R_4(\varphi)$, which corresponds to compressive region; if $R_1(\varphi) < r < R_3(\varphi)$, $\tau = R_1(\varphi)$, which corresponds to stretching region. The coordinate transformation equations are expressed by

$$x' = r'\cos(\varphi') = k_1 x + k_2 x/\sqrt{x^2 + y^2} , \quad (6)$$

$$y' = r'\sin(\varphi') = k_1 y + k_2 y/\sqrt{x^2 + y^2} \quad (7)$$

$$z' = z \quad (8)$$

with the Jacobi matrix and its determinant

$$\Lambda_i^{i'} = [A_1, A_2, 0; B_1, B_2, 0; 0, 0, 1] , \quad (9)$$

$$\det(\Lambda_i^{i'}) = A_1 B_2 - A_2 B_1 \quad (10)$$

where

$$A_1 = k_1 - a\sin\varphi\cos\varphi + (k_2/r)\sin^2\varphi - (b/r)\sin\varphi\cos\varphi ,$$

$$A_2 = a\cos^2\varphi - (k_2/r)\sin\varphi\cos\varphi + (b/r)\cos^2\varphi ,$$

$$B_1 = -a\sin^2\varphi - (k_2/r)\sin\varphi\cos\varphi - (b/r)\sin^2\varphi ,$$

$$B_2 = k_1 + a\sin\varphi\cos\varphi + (k_2/r)\cos^2\varphi + (b/r)\sin\varphi\cos\varphi ,$$

$$a = \{[\tau - R_2(\varphi)][\frac{d\tau}{d\varphi} - \frac{dR_3(\varphi)}{d\varphi}] - [\tau - R_3(\varphi)][\frac{d\tau}{d\varphi} - \frac{dR_2(\varphi)}{d\varphi}]\}/[\tau - R_2(\varphi)]^2$$

,

$$b = \{\frac{d\tau}{d\varphi}[R_3(\varphi) - R_2(\varphi)] + \tau[\frac{dR_3(\varphi)}{d\varphi} - \frac{dR_2(\varphi)}{d\varphi}]\}/[\tau - R_2(\varphi)]$$
$$-\tau[R_3(\varphi) - R_2(\varphi)][\frac{d\tau}{d\varphi} - \frac{dR_2(\varphi)}{d\varphi}]/[\tau - R_2(\varphi)]^2$$

Substituting (9) and (10) into (1), we can obtain the relative permittivity and permeability tensors of the 2D transparent device as

$$\varepsilon^{i'j'} = \mu^{i'j'} = \begin{bmatrix} \frac{A_1^2 + A_2^2}{A_1B_2 - A_2B_1} & \frac{A_1B_1 + A_2B_2}{A_1B_2 - A_2B_1} & 0 \\ \frac{A_1B_1 + A_2B_2}{A_1B_2 - A_2B_1} & \frac{B_1^2 + B_2^2}{A_1B_2 - A_2B_1} & 0 \\ 0 & 0 & \frac{1}{A_1B_2 - A_2B_1} \end{bmatrix} \quad (11)$$

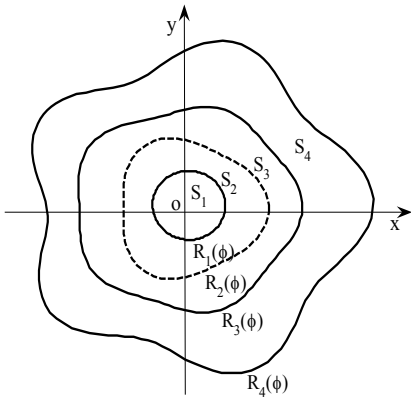

Fig.1. Schematic diagram of the space transformation for the design of arbitrary shaped 2D transparent devices.

Equation (11) gives the general expressions of the material parameters for the 2D transparent devices with non-conformal inner and outer boundaries. The permeability tensor is equal to the permittivity tensor. For special case $R_1(\varphi) = t_1 R_4(\varphi)$, $R_2(\varphi) = t_2 R_4(\varphi)$, $R_3(\varphi) = t_3 R_4(\varphi)$, where $t_i < 1$ (i = 1,2,3 and $0 < t_1 < t_2 < t_3 < 1$) represents the linear compression ratio between the inner and outer boundaries, equation (11) can be simplified as

$$\varepsilon_{x'x'} = \{[r' - \tau R(\varphi')(1-k_1)]^2\cos^2\varphi' + \tau^2(1-k_1)^2P^2\cos^2\varphi' \quad (12a)$$
$$-2\tau(1-k_1)r'P\sin\varphi'\cos\varphi' + r'^2\sin^2\varphi'\}/r'[r' - \tau R(\varphi')(1-k_1)]$$

$$\varepsilon_{y'y'} = \{[r' - \tau R(\varphi')(1-k_1)]^2\sin^2\varphi' + \tau^2(1-k_1)^2P^2\sin^2\varphi' \quad (12b)$$
$$+2\tau(1-k_1)r'P\sin\varphi'\cos\varphi' + r'^2\cos^2\varphi'\}/r'[r' - \tau R(\varphi')(1-k_1)]$$

$$\varepsilon_{x'y'} = \{-\tau R(\varphi')(1-k_1)[2r' - \tau R(\varphi')(1-k_1)]\sin\varphi'\cos\varphi' \quad (12c)$$
$$+\tau^2(1-k_1)^2P^2\sin\varphi'\cos\varphi'$$
$$+\tau(1-k_1)r'P(\cos^2\varphi' - \sin^2\varphi')\}/r'[r' - \tau R(\varphi')(1-k_1)]$$

$$\varepsilon_{z'z'} = [r' - \tau R(\varphi')(1-k_1)]/r'/k_1^2 \quad (12d)$$

$$\varepsilon_{y'x'} = \varepsilon_{x'y'} \text{ and } \varepsilon_{x'z'} = \varepsilon_{y'z'} = \varepsilon_{z'x'} = \varepsilon_{z'y'} = 0 \quad (12e)$$

For the cylindrical transparent devices with regular geometric shapes such as circular, elliptical and square, the contour equation $R_i(\varphi)$ can be simplified by the procedure illustrated in [9] to obtain the corresponding material parameters. It means that the material parameters deduced in this paper can be specialized to all formally designed 2D transparent devices with conformal inner and outer boundaries.

3. Simulation Results and Discussion

In this section, based on the finite element software COMSOL Multiphysics, we make full-wave simulation on the 2D transparent device with non-conformal inner and outer boundaries under TE wave and cylindrical wave irradiations, in order to validate the designed equation (11). To show the flexibility of the proposed approach to design cylindrical transparent device with irregular cross section, the contour equations

$$R_1(\varphi) = (12+2\cos(\varphi)+\sin(2\varphi)-2\sin(3\varphi))/320 \quad (13)$$

$$R_2(\varphi) = (20+2\sin(2\varphi)-3\sin(5\varphi)+5\cos(7\varphi))/288 \quad (14)$$

$$R_3(\varphi) = 0.175(0.8+0.1\cos(\varphi)+0.2\cos(5\varphi)+0.1\sin(5\varphi)) \quad (15)$$

$$R_4(\varphi) = (10+\sin(\varphi)-\sin(2\varphi)+2\cos(5\varphi))/48 \quad (16)$$

are chosen as an example. Since the material parameters of the 2D transparent device are independent on frequency, its performance does not vary significantly with frequency. Here, the frequency of the excitation source is set to be 2.5 GHz.

3.1 Field Distribution of the 2D Transparent Device under TE Wave Irradiation

Fig. 2(a)-(d) show the electric field distributions in the vicinity of the 2D transparent device under TE wave irradiation. The TE plane wave has an electric polarized in z direction with unit amplitude. In the simulation, perfect matched layers (PML) are applied to terminate the computational domain in $\pm x$ and $\pm y$ directions. In Fig. 2(a), the incident TE wave is from left to right along the x axis. In Fig. 2(b), the incident wave is from upside to downside along the y axis. In Fig. 2(c) and 2(d) the waves are irradiated with angles of 45° and -45°, respectively. It can be clearly seen that although the waves are distorted in the transformation region, they return to the original propagation directions and wavefronts when passing through the 2D transparent device. The performance of the device is independent on the orientation of the incident wave.

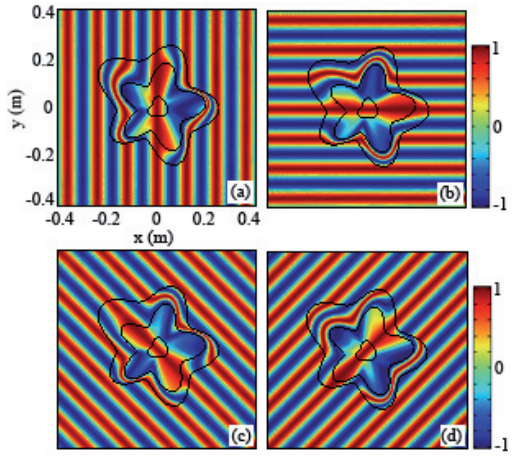

Fig.2. (Color online) The electric field (Ez) distribution in the computational domain of the 2D transparent device under TE wave irradiation.

3.2 Field Distribution of the 2D Transparent Device under Cylindrical Wave Irradiation

Since the proposed 2D transparent device has no symmetry in any direction, it's necessary to study its interaction with electromagnetic waves from different orientations. Fig. 3(a)-(d) illustrate the electric field distribution in the vicinity of the 2D transparent device under cylindrical wave irradiation, where line sources with current 10^{-3}A/m in z direction are located at (-0.35m, 0), (0, 0.35m), (-0.35m, -0.35m) and at the centre of the device, respectively. From Fig. 3(a)-(c), we can see that although the waves are distorted in the transformation region, they recovered the original propagation status when passing through the device. Interestingly, in Fig. 3(d) when the line source is located at the centre of the device, i.e., inclosed in the structure, the wavefronts of the cylindrical wave are perfectly recovered, as if the device does not exist. It indicates the effectiveness of the 2D transparent devices with arbitrary geometries in the application of optical and electromagnetic engineering.

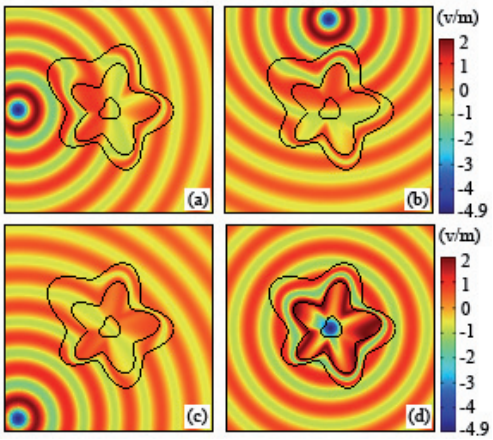

Fig.3. (Color online) The electric field distribution in the computational domain for the 2D transparent device with arbitrary geometry under cylinder wave irradiation.

3.3 Influence of Metamaterial Loss on the Performance of the 2D Transparent Device

Since metamaterials are always lossy in real applications, it does make sense to investigate the effect of loss on the transparent property of the device. The electric field in the vicinity of the 2D transparent device with electric and magnetic-loss tangents (tgδ) of 0.001, 0.005, 0.01 and 0.02 are displayed in panels (a), (b), (c) and (d) of Fig. 4, respectively. As it can be seen from Fig. 4(a) and (b) that the electric field distributions are basically undisturbed when loss tangents of 0.001 and 0.005 are added to both permittivity and permeability tensors of the anisotropic and inhomogeneous materials. When the loss tangent of the metamaterials is 0.01 or more than that, it deteriorates the

performance of the 2D transparent device, as shown in Fig. 4(c) and 4(d). The electric field distributions along the *x* axis of the 2D transparent device with electric and magnetic-loss are shown in Fig. 5. It can be seen that for the back-scattering region, performance of the 2D transparent device is independent on the loss tangent of the metamaterials. The increase of loss tangent deteriorates the performance of the 2D transparent device in the forward-scattering region of the near field. In this paper, the properties of the transparent device to TE waves are numerically verified. Since the permeability tensor is identical to the permittivity tensor, the responses of the transparent device to TM waves are the duality of their response to TE waves. Hence, the numerical results for TM cases are not included for brevity.

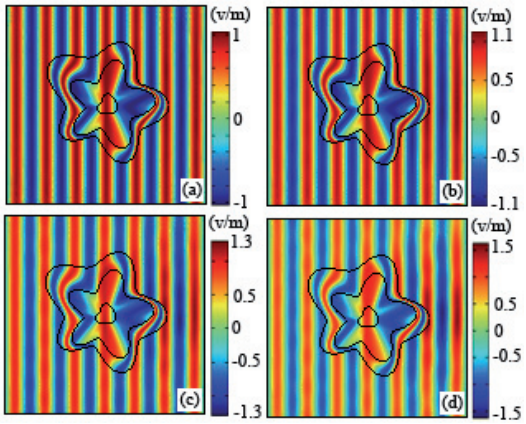

Fig.4. (Color online) The electric field (Ez) distributions in the computational domains for the 2D transparent devices with loss tangents of 0.001 (a), 0.005 (b), 0.01 (c) and 0.02(d), respectively.

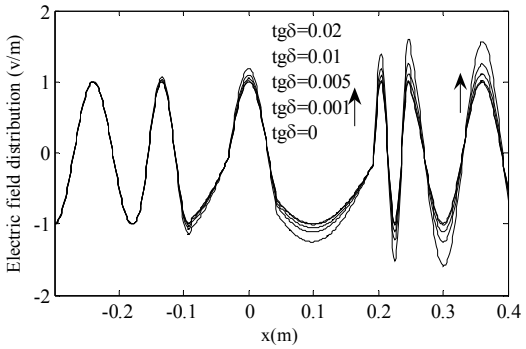

Fig. 5. The electric field distributions along x axis for the 2D transparent devices with different loss tangents.

4. Conclusions

The material parameters for 2D transparent devices with arbitrary geometries are developed. A peculiar 2D transparent device is designed as an example. All theoretical and numerical results validate the material parameters for the cylindrical transparent devices with arbitrary cross section we deduced. Besides, we have investigated the influence of metamaterial loss on the performance of the device, and found that the electric field distributions of the 2D transparent devices are basically undisturbed when loss tangent of metamaterials is less than 0.01. It is expected that our works are helpful for designing new transparent devices for antenna protection and contribute to more applications in electromagnetic field engineering.

Acknowledgements

This work was supported by the National Natural Science Foundation of China (grant no. 60861002), Training Program of Yunnan Province for Middle-aged and Young Leaders of Disciplines in Science and Technology (Grant No. 2008PY031), the Research Foundation from Ministry of Education of China (grant no. 208133), the Natural Science Foundation of Yunnan Province (grant no.2007F005M), and the National Basic Research Program of China (973 Program) (grant no. 2007CB613606).

References

[1] PENDRY, J. B., SCHURIG, D., SMITH, D. R. Controlling electromagnetic fields. *Science,* 2006, vol. 312, no. 5781, p.1780 to 1782.

[2] LEONHARDT, U. Optical conformal mapping. *Science,* 2006, vol. 312, no. 5781, p. 1777-1780.

[3] SCHURIG, D., MOCK, J. J., JUSTICE, B. J., CUMMER, S. A., PENDRY, J. B., STARR, A. F., SMITH, D. R. Metamaterial electromagnetic cloak at microwave frequencies. *Science*, 2006, vol. 314, no. 5801, p. 977-980.

[4] LEONHARDT, U., TYC, T. Broadband invisibility by non-euclidean cloaking. *Science,* 2009, vol. 323, no. 5910, p. 110-112.

[5] LIU, R., JI, C., MOCK, J. J., CHIN, J. Y., CUI, T. J., SMITH, D.R. Broadband ground-plane cloak. *Science*, vol. 323, no. 5912, p. 366-369.

[6] VALENTINE, J., LI, J., ZENTGRAF, T., BARTAL, G., ZHANG, X. An optical cloak made of dielectrics. *Nature Materials*, 2009, vol. 8, no. 7, p.568-571.

[7] ALITALO, P., TRETYAKOV, S. Electromagnetic cloaking with metamaterials. *Materials today,* 2009, vol. 12, no. 3, p. 22-29.

[8] LI, C., YAO, K., LI, F. Two-dimensional electromagnetic cloaks with non-conformal inner and outer boundaries. *Optics Express*, 2008, vol. 16, no. 23, p.19366-19374.

[9] LI, C., LI, F. Two-dimensional electromagnetic cloaks with arbitrary geometries. *Optics Express*, 2008, vol. 16, no. 17, p. 13414-13420.

[10] WU, Q., ZHANG, K., MENG, F. Y., LI, L. W. Material parameters characterization for arbitrary N-sided regular polygonal invisible cloak. *J. Appl. Phys. D: Appl. Phys.*, 2009, vol. 42, no. 3, p. 035408.

[11] LAI, Y., NG, J., CHEN, H. Y., HAN, D. Z., XIAO, J. J., ZHANG, Z. Q., CHAN, C. T. Illusion optics: the optical transformation of an object into another object. *Phys. Rev. Lett.*, 2009, vol. 102, no. 25, p. 253902.

[12] RAHM, M., SCHURIG, D., ROBERTS, D. A., CUMMER, S. A., SMITH, D. R., PENDRY, J. B. Design of electromagnetic cloaks and concentrators using form-invariant coordinate transformations

of Maxwell's equations. *Photonics and Nanostructures-Fundamentals and Applications*, 2008, vol. 6, no. 1, p. 87-95.

[13] YANG, J. J., HUANG, M., YANG, C. F., XIAO, Z., PENG, J. H. Metamaterial electromagnetic concentrators with arbitrary geometries. *Optics Express*, 2009, vol. 17, no. 22, p.19656-19661.

[14] CHEN, H., CHAN, C. T. Transformation media that rotate electromagnetic fields. *Appl. Phys. Lett.,* 2007, vol. 90, no. 24, p. 241105.

[15] GREENLEAF, A., KURYLEV, Y., LASSAS, M., UHLMANN, G. Electromagnetic wormholes and virtual magnetic monopoles from metamaterials. *Phys. Rev. Lett.*, 2007, vol. 99, no. 18, p. 183901.

[16] KILDISHEV, A. V., NARIMANOV, E. E. Impedance-matched hyperlens. *Opt. Lett.,* 2007, vol. 32, no. 23, p. 3432-3434.

[17] RAHM, M., CUMMER, S. A., SCHURIG, D., PENDRY, J. B., SMITH, D. R. Optical design of reflectionless complex media by finite embedded coordinate transformations. *Phys. Rev. Lett.*, 2008, vol. 100, no. 6, p. 063903.

[18] CHEN, H. Y., LUO, X. D., MA, H. R., CHAN, C. T. The anti-cloak. *Optic. Express*, 2008, vol. 16, no. 19, p.14603-14608.

[19] YANG, T., CHEN, H. Y., LUO, X. D., MA, H. R. Superscatterer: Enhancement of scattering with complementary media. *Optics Express*, 2008, vol. 16, no. 22, p. 18545.

[20] NG, J., CHEN, H. Y., CHAN, C. T. Metamaterial frequency-selective superabsorber. *Optics Letters*, 2009, vol. 34, no. 5, p.644-646.

[21] LAI, Y., CHEN, H. Y., ZHANG, Z. Q., CHAN, C. T. Complementary media invisibility cloak that cloaks objects at a distance outside the cloaking shell. *Phys. Rev. Lett*., 2009, vol. 102, no. 9, p. 093901.

[22] ALÙ, A., ENGHETA, N. Cloaking a sensor. *Phys. Rev. Lett*., 2009, vol. 102, no. 23, p. 233901.

[23] YU, G. X., CUI, T. J., JIANG, W. X. Design of transparent structure using metamaterial. *J. Infrared Milli Terahz Waves*, 2009, vol. 30, no. 6, p. 633-641.

[24] SCHURIG, D., PENDRY, J. B., SMITH, D. R. Calculation of material properties and ray tracing in transformation media. *Optics Express*, 2006, vol. 14, no. 21, p. 9794.

About Authors ...

Cheng-fu YANG was born in Dali Yunnan, China. He received the B.S. degree from Yunnan University. Now he is a graduate student of Yunnan University. His research interests are in the fields of electromagnetic computation and research of metamaterials.

Jing-jing YANG was born in Hekou, Yunnan, China. She received the B.S. and M.S. degrees in electric engineering from Yunnan University, Kunming, China, in 2005 and 2007, respectively. She is now a Ph.D candidate in Faculty of Materials and Metallurgical Engineering, Kunming University of Science and Technology, China. Her research interests are metamaterials, electromagnetic theory, and wireless communication.

Ming HUANG was born in Wenshan, Yunnan, China. He received the B.S. and M.S. degrees in electric engineering from Yunnan University, Kunming, China, and the Ph. D degree in microwave engineering from Kunming University of Science and Technology, China, in 1984, 1987, and 2006, respectively. His main research interests include wireless communication, microwave power application, and metamaterials. In his research area, he has (co-) authored 4 books, over 70 refereed journal papers and international conference papers. One of his research papers was highlighted by Nature China in June, 2007.

Ji-hong SHI was born in Qing Zhou, Shandong, China. She received the B.S. degree from Huazhong University of Science and Technology in 1985. Her main research interests include wireless communication, microwave power application, and metamaterials. In her research area, she has (co-) authored 4 books, over 20 refereed journal papers and international conference papers.

Jin-hui PENG was born in Mojiang, Yunnan, China. He received the B.S., M.S., and Ph.D degrees in metallurgical engineering from Kunming University of Science and Technology, China, in 1985, 1988, and 1992, respectively. His research interest is electromagnetic theory and microwave metallurgy. In his research area, he has (co-) authored 4 books, over 160 refereed journal papers. He has won many awards including the first and second Science awards of Yunnan Province, and the Gold awards of the Scientific and Technological Achievements of Young Chinese, etc.